Food and Chemical Toxicology 50 (2012) 1271–1278

Contents lists available at SciVerse ScienceDirect

Food and Chemical Toxicology

journal homepage: www.elsevier.com/locate/foodchemtox

Antitumor effects of emodin on LS1034 human colon cancer cells *in vitro* and *in vivo*: Roles of apoptotic cell death and LS1034 tumor xenografts model

Yi-Shih Ma [a,b], Shu-Wen Weng [a,c], Meng-Wei Lin [d], Chi-Cheng Lu [e], Jo-Hua Chiang [e], Jai-Sing Yang [f] Kuang-Chi Lai [g,h], Jing-Pin Lin [i], Nou-Ying Tang [i], Jaung-Geng Lin [a,*], Jing-Gung Chung [d,i,*]

[a] *Graduate Institute of Chinese Medicine, China Medical University, Taichung 404, Taiwan*
[b] *Department of Chinese Medicine, Changhua Hospital, Department of Health, Executive Yuan, Changhua 513, Taiwan*
[c] *Department of Chinese Medicine, Taichung Hospital, Department of Health, Executive Yuan, Taichung 403, Taiwan*
[d] *Department of Biological Science and Technology, China Medical University, Taichung 404, Taiwan*
[e] *Department of Life Sciences, National Chung Hsing University, Taichung 402, Taiwan*
[f] *Department of Pharmacology, China Medical University, Taichung 404, Taiwan*
[g] *School of Medicine, China Medical University, Taichung 404, Taiwan*
[h] *Department of Surgery, China Medical University Beigang Hospital, Yunlin 651, Taiwan*
[i] *Department of Biotechnology, Asia University, Taichung 413, Taiwan*

ARTICLE INFO

Article history:
Received 26 August 2011
Accepted 24 January 2012
Available online 1 February 2012

Keywords:
Emodin
Human colon cancer LS1034 cells
Apoptosis
Caspases activation
Xenograft tumor

ABSTRACT

Emodin, an active natural anthraquinone derivative, is found in the roots and rhizomes of numerous Chinese medicinal herbs and exhibits anticancer effects on many types of human cancer cell lines. The aim of this study investigated that emodin induced apoptosis of human colon cancer cells (LS1034) *in vitro* and inhibited tumor nude mice xenografts bearing LS1034 *in vivo*. In *in vitro* study, emodin induced cell morphological changes, decreased the percentage of viability, induced G2/M phase arrest and increased ROS and Ca^{2+} productions as well as loss of mitochondrial membrane potential ($\Delta\Psi_m$) in LS1034 cells. Emodin-triggered apoptosis was also confirmed by DAPI staining and these effects are concentration-dependent. Western blot analysis indicated that the protein levels of cytochrome *c*, caspase-9 and the ratio of Bax/Bcl-2 were increased in LS1034 cells after emodin exposure. Emodin induced the productions of ROS and Ca^{2+} release, and altered anti- and pro-apoptotic proteins, leading to mitochondrial dysfunction and activations of caspase-9 and caspase-3 for causing cell apoptosis. In *in vivo* study, emodin effectively suppressed tumor growth in tumor nude mice xenografts bearing LS1034. Overall, the potent *in vitro* and *in vivo* antitumor activities of emodin suggest that it might be developed for treatment of colon cancer in the future.

1. Introduction

Cancer is the major cause of death worldwide (Benson, 2007; Slattery et al., 1998). In Taiwan, based on the reports in 2009 from the Department of Health, ROC (Taiwan) indicated that 19.6 individuals per 100,000 die annually from colorectal cancer. For males and females, colon/rectum is the third leading sites among all the primary sites in Taiwan. Numerous evidences have been shown that colon cancer is largely associated with high-fat diet and causatively linked to the increased production of colonic bile acids (Chiu et al., 2003; Imray et al., 1992; Markowitz et al., 2002). The current treatment modalities are inadequate; therefore, the best strategy for chemotherapeutic agents is largely dependent on their ability to trigger cell programmed death (apoptosis) in tumor cells; therefore, novel inducers of apoptosis provide a new therapeutic approach for anti-cancer design.

It is well known that apoptosis is a highly regulated molecular mechanism for leading cells undergo programmed cell death and through the extrinsic and the intrinsic pathways (Degterev et al., 2003; Ziegler and Kung, 2008), and endoplasmic reticulum (ER) stress (Nakagawa and Yuan, 2000). The extrinsic pathway is

Abbreviations: $\Delta\Psi_m$, mitochondrial membrane potential; AIF, apoptosis-inducing factor; Bax, Bcl-2-associated X protein; Bcl-2, B-cell lymphoma 2; DAPI, 4,6-diamidino-2-phenylindole dihydrochloride; DMSO, dimethyl sulfoxide; Endo G, endonuclease G; DCFH-DA, 2′,7′-dichlorofluorescin diacetate; PI, propidium iodide.

* Corresponding authors. Address: Graduate Institute of Chinese Medicine, China Medical University, No. 91, Hsueh-Shih Road, Taichung 40402, Taiwan. Tel.: +886 422053366x3311; fax: +886 22035192 (J.-G. Lin); Department of Biological Science and Technology, China Medical University, No. 91, Hsueh-Shih Road, Taichung 40402, Taiwan. Tel.: +886 422053366x2161; fax: +886 422053764 (J.G. Chung).

E-mail addresses: jglin@mail.cmu.edu.tw (J.-G. Lin), jgchung@mail.cmu.edu.tw (J.-G. Chung).

0278-6915/$ - see front matter © 2012 Elsevier Ltd. All rights reserved.
doi:10.1016/j.fct.2012.01.033

triggered by the interaction between specific ligands and surface receptors of cells (Klein et al., 2005), the intrinsic pathway is triggered by various stimuli (DNA damage, cellular distress, hypoxia and cytotoxic agents), which act inside the cell (Degterev et al., 2003).

Emodin (1,3,8-trihydroxy-6-methyl-anthraquinone), one of major anthraquinone isolated from the root of *Rheum palmatum* L., has been shown present pharmacological function including anti-inflammatory (Chang et al., 1996), hepatoprotective (Ding et al., 2008), and anticancer activity (Yim et al., 1999). In anticancer function, numerous studies have indicated that emodin inhibits cell growth in many types of human cancer cell lines (Chen et al., 2002; Jing et al., 2002; Lai et al., 2009; Shieh et al., 2004; Srinivas et al., 2003; Zhang et al., 1998). Emodin has been demonstrated to regulate many gene expression associated with cell proliferation, cell apoptosis, oncogenesis, DNA repair and cancer cell invasion and metastasis (Cha et al., 2005; Huang et al., 2006; Kwak et al., 2006; Lu et al., 2009; Muto et al., 2007; Shieh et al., 2004). Emodin is a strong reactive oxygen species-producing agent (Jing et al., 2006) and induction of DNA damage (Wang et al., 2006). Our previous studies also showed that emodin affected the expression of cytokines and functions of leukocytes from Sprague–Dawley rats (Yu et al., 2006), and it induced apoptosis of human tongue squamous cancer SCC-4 cells through reactive oxygen species and mitochondria-dependent pathways (Lin et al., 2009). We also found that emodin has cytotoxic and protective effects in rat C6 glioma cells through the inductions of Mdr1a and nuclear factor kappa B expression (Kuo et al., 2009). There is no available information to show emodin induced apoptosis in human colon cancer cells *in vitro* and *in vivo*. Therefore, in the present study, we investigated the effects of emodin on the LS1034 human colon cancer cells *in vitro* and *in vivo*. Results indicated that emodin induced apoptosis in LS1034 cells *in vitro* and suppressed tumor nude mice xenografts bearing LS1034 *in vivo*.

2. Materials and methods

2.1. Chemicals and reagents

Emodin, propidium iodide (PI), Triton X-100, dimethyl sulfoxide (DMSO), *N*-acetylcysteine (NAC) and trypan blue were obtained from Sigma–Aldrich Corp. (St. Louis, MO, USA). RPMI 1640 medium, fetal bovine serum (FBS), L-glutamine penicillin-strptomycin and Trypsin–EDTA were obtained from Gibco/Life Technologies (Carlsbad, California, USA). Caspase-3, -8, -9 activity assay kits were bought from OncoImmunin, Inc. (Gaithersburg, MD, USA). Caspase-3 inhibitor (Z-DEVD-FMK) and caspase-9 inhibitor (Z-LEHD-FMK) were purchased from R&D systems (Minneapolis, MN, USA). The antibodies for caspase-9 and cytochrome *c* were purchased from Cell Signaling Technology (Irvine, CA, USA) and these for Bax, Bcl-2, AIF, β-actin and complex IV were obtained from Santa Cruz Biotechnology Inc. (Santa Cruz, CA, USA). Secondary antibodies conjugated with horseradish peroxidase (HRP) were bought from GE Healthcare (Piscataway, NJ, USA).

2.2. Cell culture

The human colon adenocarcinoma cell line (LS1034) was obtained from the Food Industry Research and Development Institute (Hsinchu, Taiwan). Cells were placed into 75 cm^2 tissue culture flasks and grown at 37 °C under a humidified 5% CO_2 atmosphere in RPMI 1640 medium with 2 mM L-glutamine, 10% FBS, 100 Units/ml penicillin and 100 μmg/ml streptomycin.

2.3. In vitro anticancer efficacy study

2.3.1. Cell morphological changes and viability of LS1034 cells by flow cytometry

LS1034 cells were seeded in 12-well plates at a density of 2×10^5 cells/well for 24 h. Cells were treated with various concentrations (0, 5, 10, 20, 30 and 50 μM) of emodin, while only adding 1% DMSO (solvent) for the control regimen and grown at 37 °C, 5% CO_2 and 95% air for 24 or 48 h. For morphological changes examination, cells after emodin treatment were examined and photographed under a phase contrast microscope at 200× magnification. For cell viability, cells were harvested, washed twice with phosphate-buffered saline (PBS), and re-suspended in PBS containing PI (5 μg/ml) as described elsewhere (Chiang et al., 2011; Lu et al., 2010). Cells were then determined the percentage of viability by a PI exclusion method and analyzed with a flow cytometer (Becton–Dickinson, FACSCalibur, San Jose, CA, USA) equipped with an argon ion laser for excitation at 488 nm wavelength as cited previously (Lu et al., 2010). Also, cells were pretreated with a ROS scavenger (NAC, 10 mM) for 2 h and then exposed to emodin for 24 h (Lu et al., 2010). After treatment, cells were collected and measured the viability as described above.

2.3.2. Determinations for DNA content and sub-G1 (apoptotic cells) populations

Approximately 2×10^5 cells/well of LS1034 cells in 12-well plates with 0, 10, 20, 30, 40 and 50 μM of emodin were incubated for 24 and 48 h. The cells were trypanized then harvested by centrifugation, washed with PBS and then were fixed in 70% ethanol at −20 °C overnight. Cells then were re-suspended in PBS containing 40 μg/ml PI and 0.1 mg/ml RNase A and 0.1% Triton X-100 in a dark room for 30 min at 37 °C, and analyzed by flow cytometry. Then the cell cycle distribution and sub-G1 group (apoptosis) were determined as described previously (Huang et al., 2009).

2.3.3. DAPI (4,6-diamidino-2-phenylindole dihydrochloride) staining for apoptotic cells

LS1034 cells at a density of 1×10^5 cells/well were plated in 6-well plates for 24 h and exposed to emodin (0, 10, 20, 30, 40 and 50 μM) for 24 h before cells from each treatment were isolated for DAPI staining as described previously (Chiang et al., 2011; Lu et al., 2010). After staining, the cells were examined and photographed by using a fluorescence microscope.

2.3.4. Measurements of intracellular reactive oxygen species (ROS), the levels of mitochondrial membrane potential ($\Delta\Psi_m$) and Ca^{2+} generation by flow cytometry

Approximately 2×10^5 cells/well of LS1034 cells were placed in 12-well plates and then were treated with or without 30 μM emodin for 1, 3, 6 12 or 24 h to measure the changes of ROS, $\Delta\Psi_m$ and Ca^{2+} levels. The cells were harvested, and then were re-suspended in 500 μl of DCFH-DA (Molecular Probes/Life Technologies, Eugene, OR, USA) (10 μM) for ROS, 500 μl of rhodamine 123 (1 μg/ml) (Molecular Probes) for $\Delta\Psi_m$ and 500 μl for Fluo-3/AM (2.5 μg /ml, Molecular Probes) for Ca^{2+}. Cells then were incubated at 37 °C for 30 min and analyzed by flow cytometry as previously described (Chiang et al., 2011; Ferlini and Scambia, 2007; Huang et al., 2009; Lu et al., 2010).

2.3.5. Caspase-3 and -9 activities were assayed by flow cytometry and specific caspase inhibitors pretreatment

Approximately 2×10^5 cells/well of LS1034 cells seeded in 12-well plates after pretreatment with or without both of the caspase-3 inhibitor (Z-DEVD-FMK) and caspase-9 inhibitor (Z-LEHD-FMK) for 2 h were incubated with emodin at the final concentration of 30 μM for 0, 24 and 48 h. At the end of incubation, all cells from each treatment were trypsinized and then were centrifuged, collected and washed twice with PBS. All samples were re-suspended in 50 μl of 10 μM substrate solution (PhiPhiLux-G_1D_1 for caspase-3 and CaspaLux9-M_1D_2 for caspase-9) (OncoImmunin, Inc.) before being incubated at 37 °C for 60 min. All samples were washed twice by PBS and analyzed by flow cytometry as previously described (Chiang et al., 2011; Huang et al., 2009). Cell viability was determined in emodin-treated LS1034 cells before exposure to both specific inhibitors as described elsewhere (Lu et al., 2010).

2.3.6. Protein preparation and Western blotting for examinations of the protein levels associated with apoptosis of LS1034 cells

Approximately 5×10^5 cells/well of LS1034 cells were placed in 12-well plates and then were exposed to 30 μM emodin for 0, 6, 12, 18 or 24 h. At the end of incubation, cells were trypanized, harvested and were lysed in the PRO-PREP™ protein extraction solution (iNtRON Biotechnology, Seongnam, Gyeonggi-Do, Korea). For protein determination of each sample, the cell lysates (40 μg of each) were separated by SDS–PAGE on a polyacrylamide gel followed by electrotransfer onto a PVDF membrane (Immobilon-P; Millipore, Bedford, MA, USA). The blots were then incubated with primary antibodies (1:1000 dilutions in blocking buffer) overnight at 4 °C. After being washed, secondary antibodies-conjugated with horseradish peroxidase (HRP) were applied at a dilution of 1:20,000 in blocking buffer for 1 h at room temperature. HRP-conjugated goat anti-rabbit or anti-mouse IgG (GE Healthcare, Piscataway, NJ, USA) was used as a secondary antibody for enhanced chemiluminescence (ECL Kit, Millipore, Billerica, MA, USA) as described previously (Huang et al., 2009; Wu et al., 2010). The protein levels of cytosolic and mitochondrial cytochrome *c* were carried out according to the manufacturer's protocol (Mitochondria/Cytosol Fractionation Kit, BioVision, Inc., Mountain View, CA, USA). Western blotting for examining the effects of emodin on the levels of Bax, Bcl-2, AIF, caspase-9, cytochrome *c*, β-actin and Complex IV were performed for emodin-treated LS1034 cells *in vitro* (Chiang et al., 2011; Yang et al., 2009). Relative abundance of each band was measured and evaluated by NIH ImageJ software.

2.3.7. RNA preparation and real-time polymerase chain reaction (PCR)

Approximately 1×10^6 cells/well of LS1034 cells were seeded in 6-well plates, and then were treated with 30 μM emodin for 24 and 48 h. At the end of incubation, cells were trypanized, harvested and washed twice with PBS. The total RNA from each treatment was extracted from the LS1034 cells after co-treatment with 30 μM emodin for 24 and 48 h by using a Qiagen Neasy Mini Kit (Qiagen, Inc., Valencia, CA, USA) as described previously (Chiang et al., 2011; Yu et al., 2011). High Capacity cDNA Reverse Transcription Kit (Applied Biosystems, Foster City, CA, USA)

was used for reverse transcription at 42 °C with 30 min and then add SYBR Green PCR Master Mix was added, Finally, Applied Biosystems 7300 Real-Time PCR system was performed to analyze the products by C_T method (Ji et al., 2009). The DNA sequence of primers evaluated by using the Primer Express Software was described in Table 1.

2.4. In vivo antitumor efficacy study

2.4.1. BALB/c nu/nu mice

Thirty male athymic BALB/c *nu/nu* mice at the age of 6–8 weeks were obtained from the National Laboratory Animal Center (Taipei, Taiwan) and the animals were maintained in the Laboratory Animal Center of China Medical University and taken care as the institutional guidelines (Affidavit of Approval of Animal Use Protocol, No. 97-25-N) of Institutional Animal Care and Use Committee (IACUC) of China Medical University (Taichung, Taiwan).

2.4.2. Animals' treatment

The LS1034 cells (6×10^6 cells/mouse) were subcutaneously injected into the flanks of BALB/c nu/nu mice. After tumor cell inoculation, the tumor size from each animal was measured using calipers every 3 days and calculated as previously reports as $V = L \times W^2/2$ (where V is the volume, L is the length and W is the width) with the final measurement taken for 39 days. When the tumor volume in each animal was close to 200 mm^3, then emodin treatment was started. Animals in each group were intraperitoneally injected with vehicle (1% DMSO) only, fluorouracil (5-FU) and emodin, respectively, once every 3 days at the volume of 50 μl. The whole experimental protocol was summarized in Fig. 7A. These animals with tumors were randomly divided into 3 groups. Each group contains 10 animals. Group I is the control group that was treated with vehicle (1% DMSO) only. Group II: each animal was treated with 5-FU (33 mg/kg) (Cusack et al., 2006). Group III: each animal was treated with emodin (40 mg/kg) (Cha et al., 2005; Chun-Guang et al., 2010; Huang et al., 2008). At the end of the experiment (39th day after cell inoculation), all animals from each group were anaesthetized by CO_2 and sacrificed. Tumors from each mouse were removed, measured and weighed individually as described previously (Ho et al., 2009; Su et al., 2010). Relative tumor weight (g) and inhibition rate (%) were calculated and data are expressed as mean ± S.D. ($n = 10$).

2.5. Statistical analysis

The difference between the emodin-treated and control groups were analyzed by Student's t-test, a probability of $p < 0.05$ being considered significant. In-vivo study, data are presented the mean ± SD ($n = 10$) and a value of p less than 0.05 indicates significantly different between the treated groups and analyzed by using one-way ANOVA followed by Dunnett's test.

3. Results

3.1. In vitro antitumor efficacy study

3.1.1. Effects of emodin on cell morphological changes and viability in LS1034 cells

Increasing the concentration of emodin and/or time of incubation led to increase the cell morphological changes, including cell shrinkage and blebbing (Fig. 1A) after 24-h exposure and to decrease the percentage of viable cells (Fig. 1B) for 24 and 48 h. Treatment of emodin led to more cell changed the morphology and also floated on the well compared to the control. Emodin at 50 μM significantly decreased by almost 80% the viable cells and the 50% of the viable cells were detected by the treatment of 30 μM emodin with 48-h incubation (Fig. 1B).

Table 1
The DNA sequence was evaluated using the Primer Express software in LS1034 cells after emodin for 24 and 48-h exposure.

Primer name	Primer sequence
Homo caspase-3-F	CAGTGGAGGCCGACTTCTTG
Homo caspase-3-R	TGGCACAAAGCGACTGGAT
Homo caspase-9-F	TGTCCTACTCTACTTTCCCAGGTTTT
Homo caspase-9-R	GTGAGCCCACTGCTCAAAGAT
Homo GAPDH-F	ACACCCACTCCTCCACCTTT
Homo GAPDH-R	TAGCCAAATTCGTTGTCATACC

Casapse, cysteine aspartate-specific protease; glyceraldehydes-3-phosphate dehydrogenase. Each assay was conducted at least triplicate to ensure reproducibility.

3.1.2. Effects of emodin on cell cycle arrest and apoptosis in LS1034 cells

The results from flow cytometric analysis shown in Fig. 2A and B indicated that LS1034 cells after treatment with various concentrations of emodin for 24 or 48 h increased the percentage of cells in G0/G1 by concentration-dependent (Fig. 2A and B) that indicated that emodin induced G0/G1 phase arrest. Moreover, the sub-G1 group (apoptosis) also appeared in the DNA content. Fig. 2A and B showed that when the concentration of emodin up to 30 μM caused about 30% apoptosis for a 48-h exposure which is the highest apoptosis occur in examined concentrations in LS1034 cells.

3.1.3. Effects of emodin on chromatin condensation and apoptosis in LS1034 cells

In order to further confirmed the induction of apoptosis by emodin in LS1034 cells, it was performed by flow cytometry and fluorescence photomicrographs of LS1034 cells stained with PI and DAPI, respectively, after treatment with 10–50 μM of emodin for 24 h. Results indicated that emodin at 20–50 μM induced a significant increase of sub-G1 population (apoptosis) (Fig. 3C) and condensations of nucleus (a characteristics of apoptosis) (Fig. 3D and E) in LS1034 cells and this effect is a concentration-dependent manner.

3.1.4. Effects of emodin on the levels of ROS, $\Delta\Psi_m$ and Ca^{2+} in LS1034 cells

It is well known that ROS production in cells may contribute to mitochondrial damage that may facilitate the further release of ROS into the cytoplasm (Lee et al., 2001). Investigating the possibility that the emodin-induced apoptosis in LS1034 cells could be related to contributions from the mitochondrial pathway, cells were treated with 30 μM emodin for the indicated periods of time. The results shown in Fig. 3A–C indicated that emodin treatment induced significant productions of ROS (Fig. 3A) and Ca^{2+} (Fig. 3C) release, and disruption of $\Delta\Psi m$ (Fig. 3B) in LS1034 cells. As shown in Fig. 3C, both specific inhibitors significantly increased the cell viability in comparison to emodin treatment alone LS1034 cells.

3.1.5. Effects of emodin on the activities of caspase-3 and -9 of LS1034 cells

To evaluate the effects of emodin on the activities of caspase-3 and -9 in LS1034 cells, we used flow cytometric analysis to determine the caspase activity in emodin-treated LS1034 cells. The results as can be seen in Fig. 4A indicated that emodin significantly promoted caspase-3 and -9 activities in a time-dependent manner in LS1304 cells. To investigate if emodin induces cell death through the intrinsic apoptotic signaling, cells were pretreated individually with inhibitors of caspase-3 (Z-DEVD-FMK) and caspase-9 (Z-LEHD-FMK) before 30 μM emodin for a 24-h treatment. Fig. 4B indicates that both specific inhibitors significantly increased the cell viability in comparison to emodin treatment alone LS1034 cells.

3.1.6. Western blotting for examining the levels of proteins associated with apoptosis in LS1034 cells

To confirm that the effect of emodin induced cell death in LS1034 cells as noted in flow cytometric assays was due to apoptosis, LS1034 cells were cultured for 0, 6, 12, 24, and 48 h with or without 30 μM emodin treatment. Cells were harvested from each treatment and then were lysed and total proteins from each sample were prepared for Western blotting analysis for apoptosis-associated proteins expression. The results from Western blots are shown in Fig. 5A and B and indicated that the levels of Bax, caspase-9, cytosolic cytochrome *c* and AIF were increased and

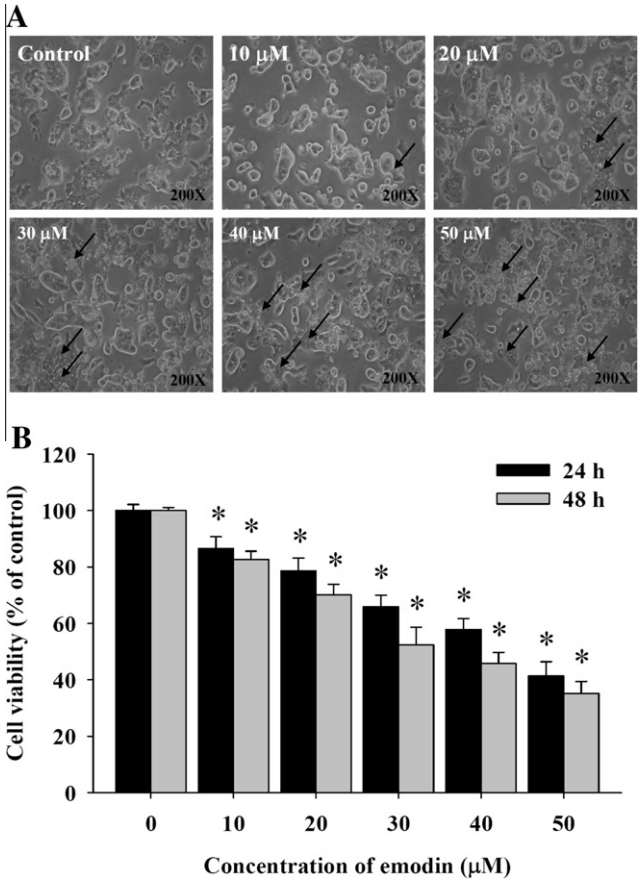

Fig. 1. Emodin induced cells' morphological changes and decreased the total viable LS1034 human colon cancer cells. Cells were incubated with or without 0, 10, 20, 30, and 50 μM of emodin for 24 h or 48 h, and then were examined and photographed by a phase-contrast microscope (A) and were harvested for determination the percentage of viable cells by flow cytometry (B) as described in Section 2. Data represents mean ± S.D. of three experiments. $^{*}p < 0.05$ was significantly different from the control sample (0 μM emodin).

the level of Bcl-2 was decreased, which led to cell apoptosis in emodin-treated LS1034 cells.

3.1.7. Effects of emodin on the mRNA expressions of caspase-3 and -9 in LS1034 cells

After 30 μM emodin treatment in LS1034 cells for 0, 24 and 48-h incubation, cells were collected and total RNA from each sample were isolated and then real-time PCR was used for gene expression of the mRNA levels of caspase-3 and -9. The gene levels of *caspase-3* and *caspase-9* elevated at 24- and 48-h exposure when compared with the control sample as can be seen in Fig. 6.

3.1.8. In vivo antitumor efficacy study

The results from *in vitro* experiments indicated that emodin induced cytotoxic effects in LS1034 cells through the G0/G1 phase arrest and induction of apoptosis. Herein, we investigated whether or not emodin affected the xenografts colon tumor *in vivo*. Thus, we further examined the effects of emodin on *in vivo* tumor growth for 39 days in a LS1034 tumor xenograft model *in vivo*. Mice after exposure to 5-FU (33 mg/kg) were acted as a positive control. Tumor size in the vehicle control group increased four folds over a period of 5 weeks when compared to the 15th day after cell inoculation. Emodin (40 mg/kg) treatment once every 3 days resulted in a decrease of tumor weight (Fig. 7C) and tumor volume (Fig. 7D), and respective

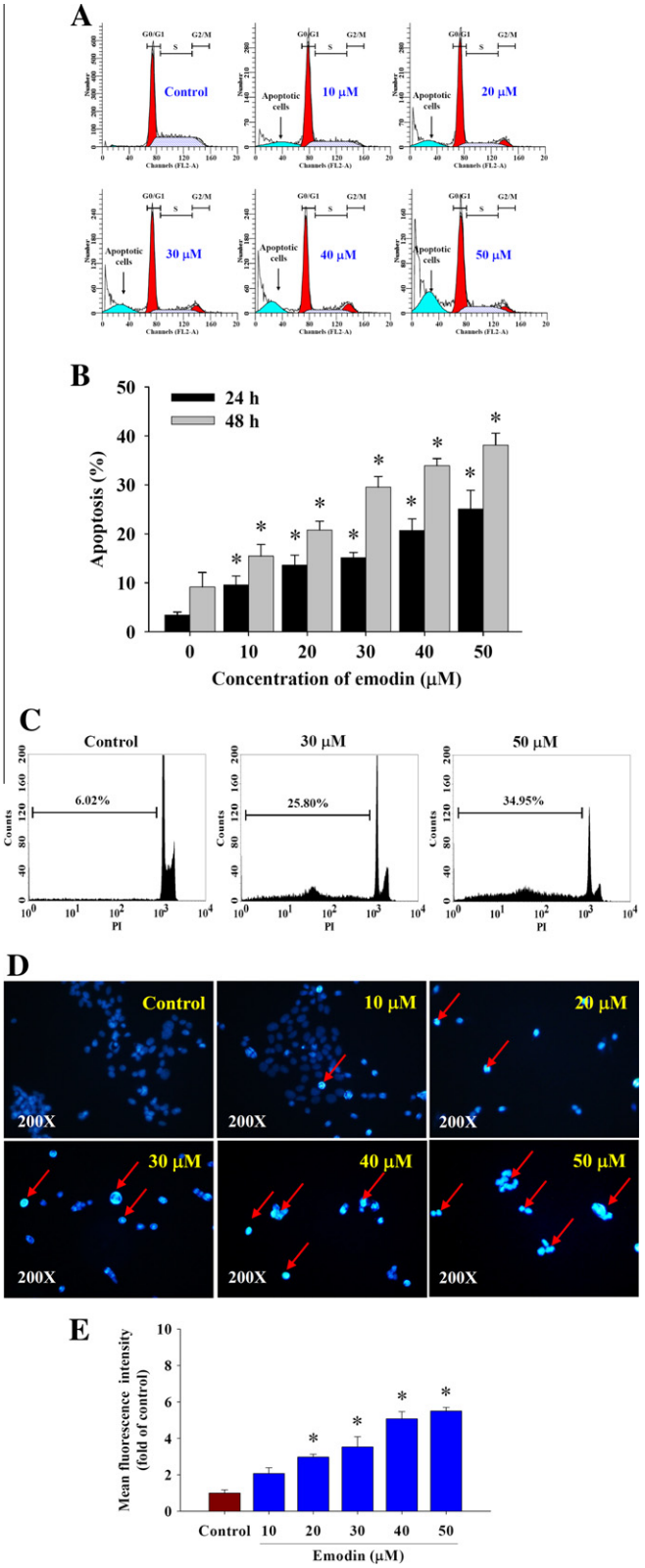

Fig. 2. Emodin changed the DNA content and induced apoptosis in LS1034 cells. Cells were incubated with or without 0, 10, 20, 30, 40 or 50 μM of emodin for 24 and 48 h, and then were harvested for determination the distribution of cell cycle for 24 h-treatment (A), sub-G1 phase (apoptosis) (B) and DNA content of apoptotic in emodin-treated LS1034 cells for 48-h exposure (C) by flow cytometry. DAPI staining (D) and quantitied results (E) were expressed as described in Section 2. Data represents mean ± S.D. of three experiments. $*p < 0.05$ shows significantly different from the control sample (0 μM emodin).

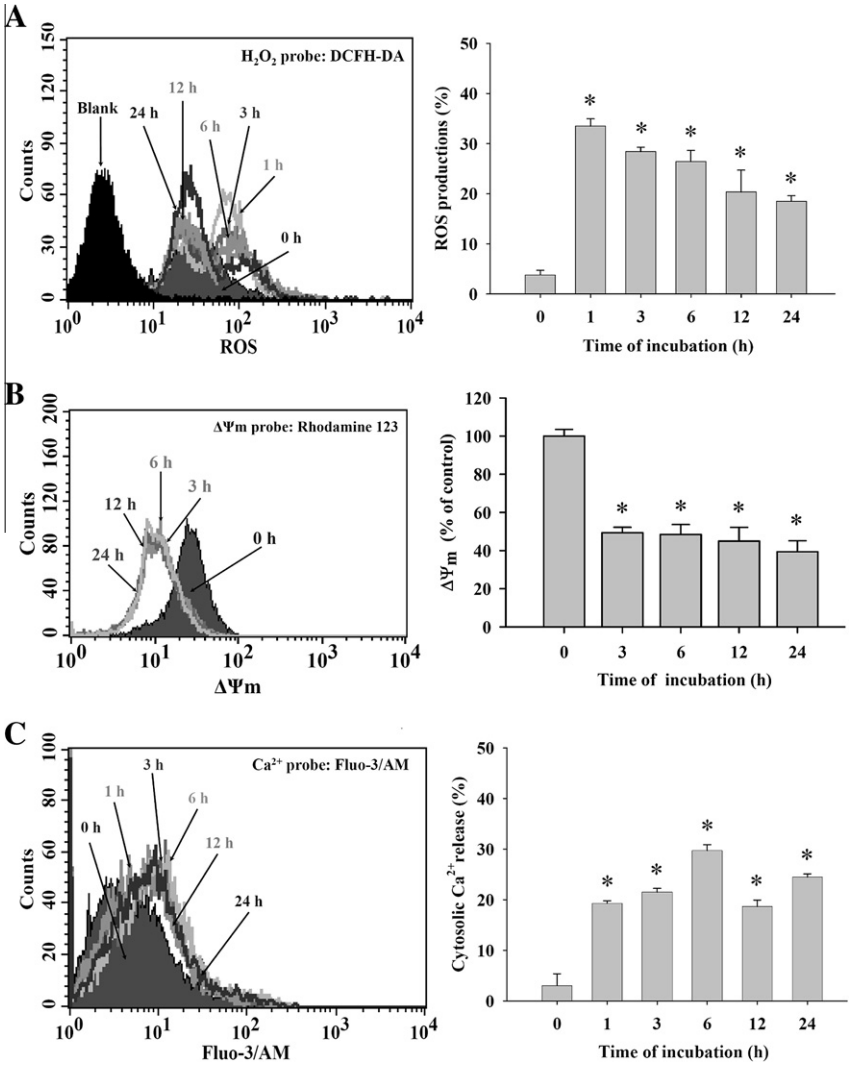

Fig. 3. Emodin affected the levels of productions of reactive oxygen species (ROS), mitochondrial membrane potential ($\Delta\Psi_m$) and Ca^{2+} in LS1034 cells. Cells were treated with 30 μM emodin for various time periods (1, 3, 6, 12 or 24 h), and then were collected. Cells were stained with DCFH-DA for ROS production (A), rhodamine 123 for the $\Delta\Psi_m$ level (B) and Fluo-3/AM for Ca^{2+} level (C) and determined by flow cytometry as described in Section 2.*$p < 0.05$, significantly different between control and emodin-treated groups.

solid tumor (Fig. 7A) in comparison to the control group. The inhibition rate of LS10345 xenografts tumor was shown that 46% T/C (the treated-group (T) over control (C) tumor volume ratio × 100%) (Table 2) when compared with the control group.

4. Discussion

Emodin has been isolated from various Chinese medicinal plants such as *Rheum palmatum* L. and it has been shown to present biological function including anticancer activities in many human cancer cells. In the present investigation, we observed that emodin inhibited the growth of human colon cancer cells (LS1034) *in vitro* through the G0/G1 phase arrest and induction of apoptosis. The molecular mechanism of emodin induced cell apoptosis through the increase the ROS and Ca^{2+} production and induced mitochondrial dysfunction (loss of the $\Delta\Psi_m$ level) which also caused by the changes of ratio of Bxa/Bcl-2. Furthermore, in the present studies, we also found that emodin inhibited the LS1034 tumor xenograft mice *in vivo*.

Herein, we found that emodin induced cell morphological changes and decreased the percentage of viable LS1034 cells and these effects are a concentration-dependent manner (Fig. 1A and B) which is in agreement with other reports showed that emodin induced cytotoxic effects in human prostate cancer LNCaP cells (Yu et al., 2008). Results from flow cytometric assay also showed that emodin promoted G0/G1 phase arrest and induced sub-G1 phase in cell cycle distribution of LS1034 cells (Fig. 2A and B) which is in agreement with previous report addressing anticancer effects in human prostate cancer cells (Yu et al., 2008).

It is well documented that apoptosis is a programmed and physiological mode of cell death. The characters of apoptosis including cell morphological change and extensive DNA fragmentation and apoptotic body, which are triggered by apoptosis-inducing signal and the frequency and time of appearance of which depend on the cell line (Arends et al., 1990; Bortner et al., 1995). If the cells did not go through apoptosis which may promote survival and accumulation of cells to form tumor (Hoeppner et al., 1996). Therefore, it was suggested that apoptosis has become a target for eliminating cancer cells (Hong and Sporn, 1997; Kelloff et al., 2000). To examine the effects of emodin on apoptosis in LS1034 colon cancer cells *in vitro*, flow cytometric assay and DAPI staining were used to study the sub-G1 phase of cell cycle, morphological changes and DNA condensation, respectively (Fig. 2C and D). Our results indicate

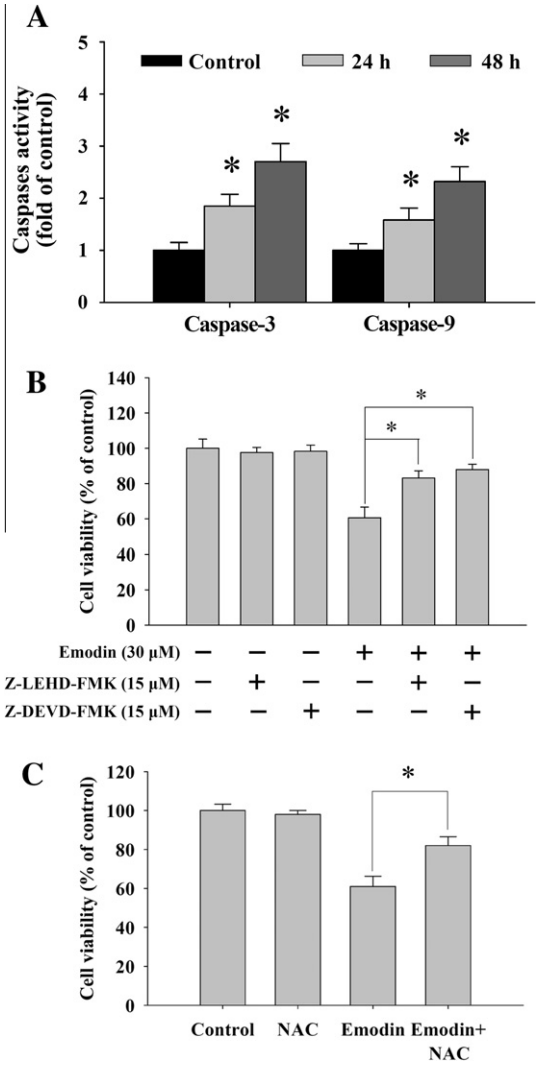

Fig. 4. Emodin stimulated caspase-3, -8 and -9 activities and altered viability after pre-incubation with specific inhibitors in LS1034 cells. (A) Cells were treated with 30 μM emodin for 24 and 48 h, and then were collected for determining activities of caspase-3 and -9 by using PhiPhiLux™-G_1D_2 and CaspaLux™9-M_1D_2 Kits (OncoImmunin, Inc.) as described in Section 2. (B) Cells were incubated with 30 μM emodin for 24 h before exposure in presence and absence of the specific inhibitors of caspase-3 (Z-DEVD-FMK) and caspase-9 (Z-LEHD-FMK) for 2 h to measure the viability in LS1034 cells. Data represents mean ± S.D. of three experiments. $^{*}p < 0.05$ shows significant difference compared with the control group.

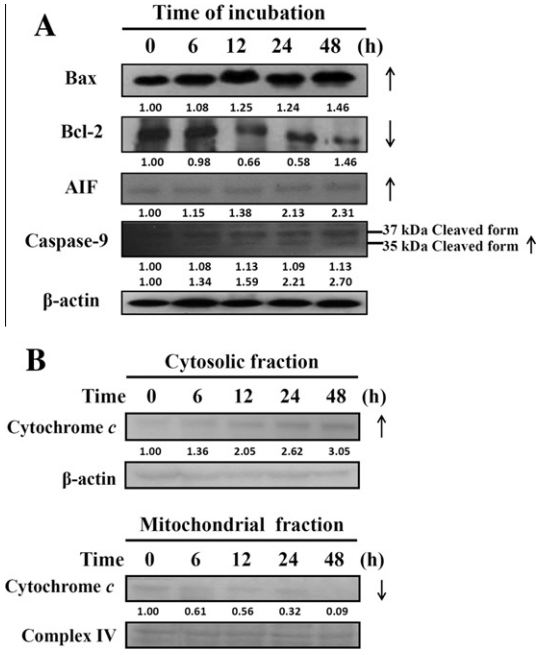

Fig. 5. Emodin affected the apoptosis-associated protein levels on LS1034 cells. Cells were incubated with or without 30 μM emodin for 0, 6, 12, 24 and 48 h, and the cells were collected for Western blotting as described in Section 2. (A) The protein levels of Bax, Bcl-2, AIF and caspase-9 were shown and (B) the fractionate cytosolic (top) and mitochondrial (bottom) cellular cytochrome *c* protein were performed. The use of β-actin and complex IV are as an internal control, respectively.

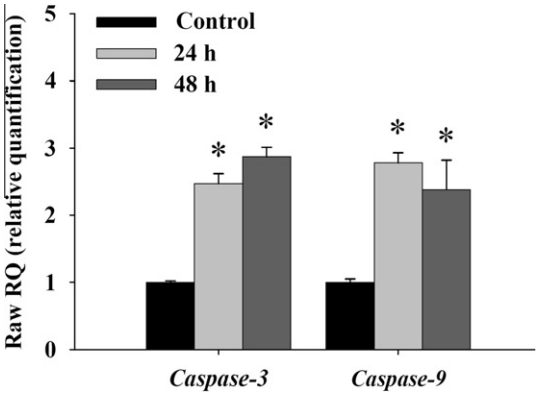

Fig. 6. Emodin enhanced the mRNA gene expression of caspase-3 and -9 in LS1034 cells. Cells were treated with or without 30 μM emodin for 24 and 48 h, and then cells were harvested for isolation of total RNA then for real-time PCR to examine the gene expression of caspase-3 and -9 as described in Materials and Methods. Data represents mean ± S.D. of three experiments. $^{*}p < 0.05$ and $^{***}p < 0.001$ were considered significant when compared with the control sample.

Table 2
Representative LS1034 xenograft tumor weight and rate of inhibition (%) after intraperitoneal injected with emodin and 5-FU.

Treatment dosage	Tumor weight (g)	Inhibition rate (%)
5-FU 33 mg/kg	0.51 ± 0.026	46.47
Control	0.95 ± 0.126	–
Emodin 40 mg/kg	0.55 ± 0.240	42.32

that emodin induced LS1034 cell apoptosis, in good agreement with the DAPI staining results showing apoptosis in human prostate cancer cells treated with emodin (Yu et al., 2008). Results from DAPI staining (Fig. 2D and E) showed that the nuclear morphology changed dramatically after emodin treatment. These observations indicated that the nuclear morphology change *s* and DNA damages occurred in the cell apoptotic process of LS1034 cells. Alternatively, we found that emodin induced production of ROS for causing cell apoptosis in LS1034 cells (Fig. 3A). *N*-acetylcysteine (NAC, a ROS scavenger) can decrease emodin-induced cell death when compared with emodin-treated cells alone (Fig. 4C) and this result is in agreement with several other reports (Chang et al., 2011; Su et al., 2005; Wang et al., 2011).

It is reported that apoptosis can be divided into mitochondria-dependent and -independent pathways. Furthermore, it was reported that if the loss of the outer mitochondrial membrane integrity and the release of cytochrome *c* from the mitochondria to the cytosol of cells after exposed stimulator then the cells are committed to apoptosis (Di Giovanni et al., 2001; Lee et al., 2001). In the present study, our results already showed that emodin decreased the levels

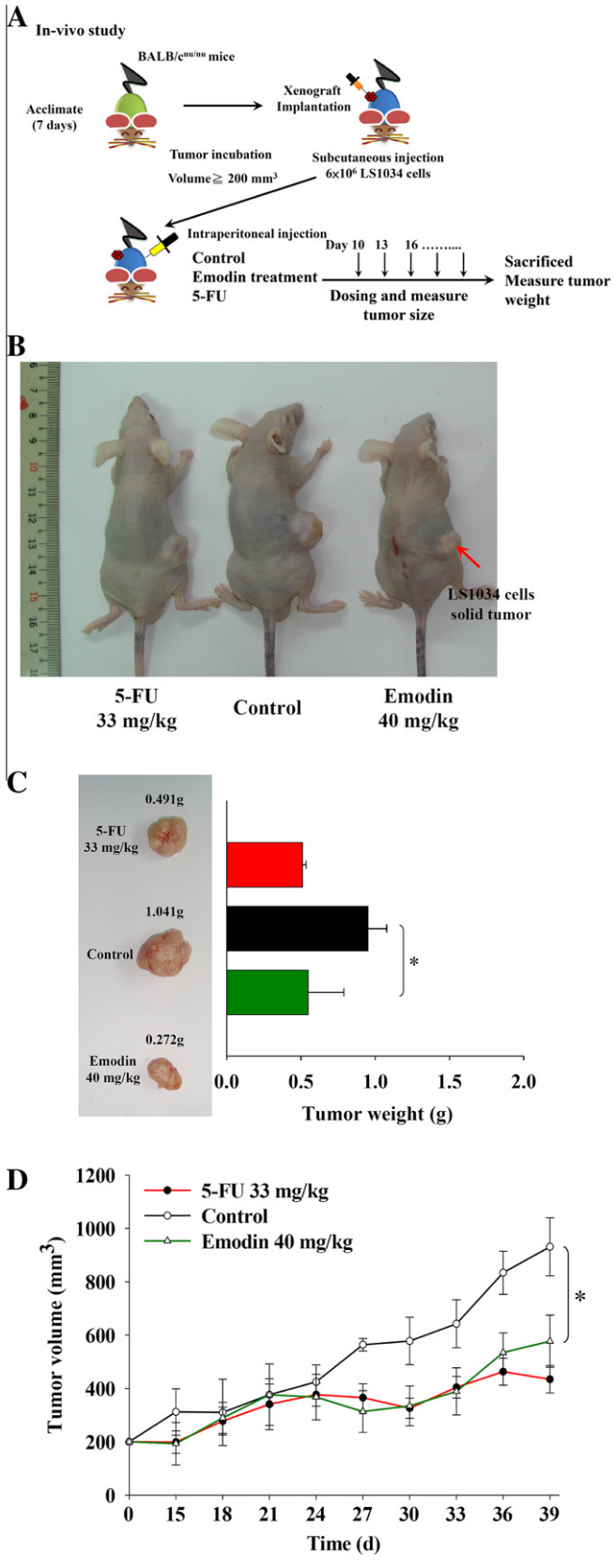

Fig. 7. Emodin suppressed tumor nude mice xenografts bearing LS1034. (A) The whole *in vivo* experimental protocol was summarized. (B) Illustration of a representative tumor after treatment with emodin and control. (C) The effect of emodin and 5-FU tumor weight and (D) the effect of emodin and 5-FU on tumor size. Data presented are the mean ± S.D. ($n = 10$) at 15–39 days post-tumor implantation and the groups were compared and analyzed by using one-way ANOVA followed by Dunnett's test. $^{*}p < 0.05$, significantly different.

of $\Delta\Psi_m$ of LS1034 cells (Fig. 3B) and this effect is time-dependent. Alternatively, the activities of caspase-3 and -9 (Fig. 4A) were stimulated, and the gene expression levels of *caspase-3* and *caspase-9* (Fig. 6) were also promoted in emodin-treated LS1034 cells. We also used caspase-3 and -9 specific inhibitors (Z-DEVD-FMK and Z-LEHD-FMK, respectively) to confirm this signaling in this investigation (Fig. 4B). However, emodin did not affect gene expression level of *caspse-8* in LS1034 cells (data not shown). Thus, we suggest that emodin-induced apoptosis in LS1034 cells may be mediated through a mitochondria-dependent pathway.

In order to investigate the possible molecular signal pathway of apoptosis in LS1034 cells after exposure to emodin, Western blotting analysis was used for examining the apoptotic protein levels, which indicated that anti-apoptotic Bcl-2 significantly decrease in comparison to control cells ($p < 0.05$) and pro-apoptotic Bax was significantly increase in comparison to control cells ($p < 0.05$) (Fig. 5A) which led to the decrease the ratio of Bax/Bcl-2 then caused mitochondrial dysfunction then induced apoptosis. It was reported that Bax/Bcl-2 ratio indicates whether and how a cell will respond to an apoptotic signal (Yang et al., 2010). Our results showed that the Bcl-2/Bax ratio therefore decreased with increasing emodin concentration. This decrease may contribute to the activation of caspase-3 and induction of apoptosis *via* the mitochondrial apoptosis pathway.

The results from the *in vivo* experiment (LS1034 tumor xenograft mice model) showed that the tumor grew faster in DMSO control group; however, slower in 5-FU and emodin-treated groups. Both the tumor volumes and weights in the 5-FU and emodin-treated groups were significantly smaller than those in the DMSO group following 39 days.

In conclusion, we found that emodin induced cell death through promoting the cell cycle arrest and apoptosis in human colon cancer LS1034 cells *in vitro* and *in vivo*. Thus, we proposed that emodin treatment results primarily in caspase-dependent death, a mechanism eliciting much current interest with respect to its therapeutic potential in colon cancer in the future. Furthermore, emodin inhibited tumor nude mice xenografts bearing LS1034 *in vivo*. These findings may aid in the understanding of the mode of actions of the emodin and provide a theoretical basis for the therapeutic use of this compound in further investigations.

Conflict of Interest

None declared.

Acknowledgements

This study is supported by the research Grant CMU97-163 from China Medical University, Taichung, Taiwan.

References

Arends, M.J., Morris, R.G., Wyllie, A.H., 1990. Apoptosis. The role of the endonuclease. Am. J. Pathol. 136, 593–608.
Benson III, A.B., 2007. Epidemiology, disease progression, and economic burden of colorectal cancer. J. Manag. Care Pharm. 13, S5–S18.
Bortner, C.D., Oldenburg, N.B., Cidlowski, J.A., 1995. The role of DNA fragmentation in apoptosis. Trends Cell Biol. 5, 21–26.
Cha, T.L., Qiu, L., Chen, C.T., Wen, Y., Hung, M.C., 2005. Emodin down-regulates androgen receptor and inhibits prostate cancer cell growth. Cancer Res. 65, 2287–2295.
Chang, C.H., Lin, C.C., Yang, J.J., Namba, T., Hattori, M., 1996. Anti-inflammatory effects of emodin from ventilago leiocarpa. Am. J. Chin. Med. 24, 139–142.
Chang, Y.C., Lai, T.Y., Yu, C.S., Chen, H.Y., Yang, J.S., Chueh, F.S., Lu, C.C., Chiang, J.H., Huang, W.W., Ma, C.Y., Chung, J.G., 2011. Emodin induces apoptotic death in murine myelomonocytic leukemia WEHI-3 cells in vitro and enhances phagocytosis in leukemia mice in vivo. Evid. Based Complement Alternat. Med. 2011, 523596.
Chen, Y.C., Shen, S.C., Lee, W.R., Hsu, F.L., Lin, H.Y., Ko, C.H., Tseng, S.W., 2002. Emodin induces apoptosis in human promyeloleukemic HL-60 cells

accompanied by activation of caspase 3 cascade but independent of reactive oxygen species production. Biochem. Pharmacol. 64, 1713–1724.
Chiang, J.H., Yang, J.S., Ma, C.Y., Yang, M.D., Huang, H.Y., Hsia, T.C., Kuo, H.M., Wu, P.P., Lee, T.H., Chung, J.G., 2011. Danthron, an anthraquinone derivative, induces DNA damage and caspase cascades-mediated apoptosis in SNU-1 human gastric cancer cells through mitochondrial permeability transition pores and Bax-triggered pathways. Chem. Res. Toxicol. 24, 20–29.
Chiu, B.C., Ji, B.T., Dai, Q., Gridley, G., McLaughlin, J.K., Gao, Y.T., Fraumeni Jr., J.F., Chow, W.H., 2003. Dietary factors and risk of colon cancer in Shanghai, China. Cancer Epidemiol. Biomarkers Prev. 12, 201–208.
Chun-Guang, W., Jun-Qing, Y., Bei-Zhong, L., Dan-Ting, J., Chong, W., Liang, Z., Dan, Z., Yan, W., 2010. Anti-tumor activity of emodin against human chronic myelocytic leukemia K562 cell lines in vitro and in vivo. Eur. J. Pharmacol. 627, 33–41.
Cusack Jr., J.C., Liu, R., Xia, L., Chao, T.H., Pien, C., Niu, W., Palombella, V.J., Neuteboom, S.T., Palladino, M.A., 2006. NPI-0052 enhances tumoricidal response to conventional cancer therapy in a colon cancer model. Clin. Cancer Res. 12, 6758–6764.
Degterev, A., Boyce, M., Yuan, J., 2003. A decade of caspases. Oncogene 22, 8543–8567.
Di Giovanni, S., Mirabella, M., Papacci, M., Odoardi, F., Silvestri, G., Servidei, S., 2001. Apoptosis and ROS detoxification enzymes correlate with cytochrome *c* oxidase deficiency in mitochondrial encephalomyopathies. Mol. Cell. Neurosci. 17, 696–705.
Ding, Y., Zhao, L., Mei, H., Zhang, S.L., Huang, Z.H., Duan, Y.Y., Ye, P., 2008. Exploration of Emodin to treat alpha-naphthylisothiocyanate-induced cholestatic hepatitis via anti-inflammatory pathway. Eur. J. Pharmacol. 590, 377–386.
Ferlini, C., Scambia, G., 2007. Assay for apoptosis using the mitochondrial probes, Rhodamine123 and 10-*N*-nonyl acridine orange. Nat. Protoc. 2, 3111–3114.
Ho, Y.T., Yang, J.S., Lu, C.C., Chiang, J.H., Li, T.C., Lin, J.J., Lai, K.C., Liao, C.L., Lin, J.G., Chung, J.G., 2009. Berberine inhibits human tongue squamous carcinoma cancer tumor growth in a murine xenograft model. Phytomedicine 16, 887–890.
Hoeppner, D.J., Hengartner, M.O., Fisher, D.E., 1996. Programmed cell death: from development to disease. Meeting report. Biochim. Biophys. Acta 1242, 217–220.
Hong, W.K., Sporn, M.B., 1997. Recent advances in chemoprevention of cancer. Science 278, 1073–1077.
Huang, Q., Shen, H.M., Shui, G., Wenk, M.R., Ong, C.N., 2006. Emodin inhibits tumor cell adhesion through disruption of the membrane lipid Raft-associated integrin signaling pathway. Cancer Res. 66, 5807–5815.
Huang, S.P., Chen, J.C., Wu, C.C., Chen, C.T., Tang, N.Y., Ho, Y.T., Lo, C., Lin, J.P., Chung, J.G., Lin, J.G., 2009. Capsaicin-induced apoptosis in human hepatoma HepG2 cells. Anticancer Res. 29, 165–174.
Huang, X.Z., Wang, J., Huang, C., Chen, Y.Y., Shi, G.Y., Hu, Q.S., Yi, J., 2008. Emodin enhances cytotoxicity of chemotherapeutic drugs in prostate cancer cells: the mechanisms involve ROS-mediated suppression of multidrug resistance and hypoxia inducible factor-1. Cancer Biol. Ther. 7, 468–475.
Imray, C.H., Radley, S., Davis, A., Barker, G., Hendrickse, C.W., Donovan, I.A., Lawson, A.M., Baker, P.R., Neoptolemos, J.P., 1992. Faecal unconjugated bile acids in patients with colorectal cancer or polyps. Gut 33, 1239–1245.
Ji, B.C., Hsu, W.H., Yang, J.S., Hsia, T.C., Lu, C.C., Chiang, J.H., Yang, J.L., Lin, C.H., Lin, J.J., Suen, L.J., Gibson Wood, W., Chung, J.G., 2009. Gallic acid induces apoptosis via caspase-3 and mitochondrion-dependent pathways in vitro and suppresses lung xenograft tumor growth in vivo. J. Agric. Food Chem. 57, 7596–7604.
Jing, X., Ueki, N., Cheng, J., Imanishi, H., Hada, T., 2002. Induction of apoptosis in hepatocellular carcinoma cell lines by emodin. Jpn. J. Cancer Res. 93, 874–882.
Jing, Y., Yang, J., Wang, Y., Li, H., Chen, Y., Hu, Q., Shi, G., Tang, X., Yi, J., 2006. Alteration of subcellular redox equilibrium and the consequent oxidative modification of nuclear factor kappaB are critical for anticancer cytotoxicity by emodin, a reactive oxygen species-producing agent. Free Radic. Biol. Med. 40, 2183–2197.
Kelloff, G.J., Crowell, J.A., Steele, V.E., Lubet, R.A., Malone, W.A., Boone, C.W., Kopelovich, L., Hawk, E.T., Lieberman, R., Lawrence, J.A., Ali, I., Viner, J.L., Sigman, C.C., 2000. Progress in cancer chemoprevention: development of diet-derived chemopreventive agents. J. Nutr. 130, 467S–471S.
Klein, S., McCormick, F., Levitzki, A., 2005. Killing time for cancer cells. Nat. Rev. Cancer 5, 573–580.
Kuo, T.C., Yang, J.S., Lin, M.W., Hsu, S.C., Lin, J.J., Lin, H.J., Hsia, T.C., Liao, C.L., Yang, M.D., Fan, M.J., Wood, W.G., Chung, J.G., 2009. Emodin has cytotoxic and protective effects in rat C6 glioma cells: roles of Mdr1a and nuclear factor kappaB in cell survival. J. Pharmacol. Exp. Ther. 330, 736–744.
Kwak, H.J., Park, M.J., Park, C.M., Moon, S.I., Yoo, D.H., Lee, H.C., Lee, S.H., Kim, M.S., Lee, H.W., Shin, W.S., Park, I.C., Rhee, C.H., Hong, S.I., 2006. Emodin inhibits vascular endothelial growth factor-A-induced angiogenesis by blocking receptor-2 (KDR/Flk-1) phosphorylation. Int. J. Cancer 118, 2711–2720.
Lai, J.M., Chang, J.T., Wen, C.L., Hsu, S.L., 2009. Emodin induces a reactive oxygen species-dependent and ATM-p53-Bax mediated cytotoxicity in lung cancer cells. Eur. J. Pharmacol. 623, 1–9.
Lee, M.G., Lee, K.T., Chi, S.G., Park, J.H., 2001. Costunolide induces apoptosis by ROS-mediated mitochondrial permeability transition and cytochrome *C* release. Biol. Pharm. Bull. 24, 303–306.
Lin, S.Y., Lai, W.W., Ho, C.C., Yu, F.S., Chen, G.W., Yang, J.S., Liu, K.C., Lin, M.L., Wu, P.P., Fan, M.J., Chung, J.G., 2009. Emodin induces apoptosis of human tongue squamous cancer SCC-4 cells through reactive oxygen species and mitochondria-dependent pathways. Anticancer Res. 29, 327–335.
Lu, C.C., Yang, J.S., Huang, A.C., Hsia, T.C., Chou, S.T., Kuo, C.L., Lu, H.F., Lee, T.H., Wood, W.G., Chung, J.G., 2010. Chrysophanol induces necrosis through the production of ROS and alteration of ATP levels in J5 human liver cancer cells. Mol. Nutr. Food Res. 54, 967–976.
Lu, H.F., Lai, K.C., Hsu, S.C., Lin, H.J., Kuo, C.L., Liao, C.L., Yang, J.S., Chung, J.G., 2009. Involvement of matrix metalloproteinases on the inhibition of cells invasion and migration by emodin in human neuroblastoma SH-SY5Y cells. Neurochem. Res. 34, 1575–1583.
Markowitz, S.D., Dawson, D.M., Willis, J., Willson, J.K., 2002. Focus on colon cancer. Cancer Cell 1, 233–236.
Muto, A., Hori, M., Sasaki, Y., Saitoh, A., Yasuda, I., Maekawa, T., Uchida, T., Asakura, K., Nakazato, T., Kaneda, T., Kizaki, M., Ikeda, Y., Yoshida, T., 2007. Emodin has a cytotoxic activity against human multiple myeloma as a Janus-activated kinase 2 inhibitor. Mol. Cancer Ther. 6, 987–994.
Nakagawa, T., Yuan, J., 2000. Cross-talk between two cysteine protease families. Activation of caspase-12 by calpain in apoptosis. J. Cell. Biol. 150, 887–894.
Shieh, D.E., Chen, Y.Y., Yen, M.H., Chiang, L.C., Lin, C.C., 2004. Emodin-induced apoptosis through p53-dependent pathway in human hepatoma cells. Life Sci. 74, 2279–2290.
Slattery, M.L., Boucher, K.M., Caan, B.J., Potter, J.D., Ma, K.N., 1998. Eating patterns and risk of colon cancer. Am. J. Epidemiol. 148, 4–16.
Srinivas, G., Anto, R.J., Srinivas, P., Vidhyalakshmi, S., Senan, V.P., Karunagaran, D., 2003. Emodin induces apoptosis of human cervical cancer cells through poly(ADP-ribose) polymerase cleavage and activation of caspase-9. Eur. J. Pharmacol. 473, 117–125.
Su, C.C., Yang, J.S., Lu, C.C., Chiang, J.H., Wu, C.L., Lin, J.J., Lai, K.C., Hsia, T.C., Lu, H.F., Fan, M.J., Chung, J.G., 2010. Curcumin inhibits human lung large cell carcinoma cancer tumour growth in a murine xenograft model. Phytother. Res. 24, 189–192.
Su, Y.T., Chang, H.L., Shyue, S.K., Hsu, S.L., 2005. Emodin induces apoptosis in human lung adenocarcinoma cells through a reactive oxygen species-dependent mitochondrial signaling pathway. Biochem. Pharmacol. 70, 229–241.
Wang, L., Lin, L., Ye, B., 2006. Electrochemical studies of the interaction of the anticancer herbal drug emodin with DNA. J. Pharm. Biomed. Anal. 42, 625–629.
Wang, W., Sun, Y., Li, X., Li, H., Chen, Y., Tian, Y., Yi, J., Wang, J., 2011. Emodin potentiates the anticancer effect of cisplatin on gallbladder cancer cells through the generation of reactive oxygen species and the inhibition of survivin expression. Oncol. Rep. 26, 1143–1148.
Wu, S.H., Hang, L.W., Yang, J.S., Chen, H.Y., Lin, H.Y., Chiang, J.H., Lu, C.C., Yang, J.L., Lai, T.Y., Ko, Y.C., Chung, J.G., 2010. Curcumin induces apoptosis in human non-small cell lung cancer NCI-H460 cells through ER stress and caspase cascade- and mitochondria-dependent pathways. Anticancer Res. 30, 2125–2133.
Yang, J.S., Chen, G.W., Hsia, T.C., Ho, H.C., Ho, C.C., Lin, M.W., Lin, S.S., Yeh, R.D., Ip, S.W., Lu, H.F., Chung, J.G., 2009. Diallyl disulfide induces apoptosis in human colon cancer cell line (COLO 205) through the induction of reactive oxygen species, endoplasmic reticulum stress, caspases casade and mitochondrial-dependent pathways. Food Chem. Toxicol. 47, 171–179.
Yang, J.S., Hour, M.J., Huang, W.W., Lin, K.L., Kuo, S.C., Chung, J.G., 2010. MJ-29 inhibits tubulin polymerization, induces mitotic arrest, and triggers apoptosis via cyclin-dependent kinase 1-mediated Bcl-2 phosphorylation in human leukemia U937 cells. J. Pharmacol. Exp. Ther. 334, 477–488.
Yim, H., Lee, Y.H., Lee, C.H., Lee, S.K., 1999. Emodin, an anthraquinone derivative isolated from the rhizomes of Rheum palmatum, selectively inhibits the activity of casein kinase II as a competitive inhibitor. Planta Med. 65, 9–13.
Yu, C.X., Zhang, X.Q., Kang, L.D., Zhang, P.J., Chen, W.W., Liu, W.W., Liu, Q.W., Zhang, J.Y., 2008. Emodin induces apoptosis in human prostate cancer cell LNCaP. Asian J. Androl. 10, 625–634.
Yu, F.S., Yang, J.S., Yu, C.S., Lu, C.C., Chiang, J.H., Lin, C.W., Chung, J.G., 2011. Safrole induces apoptosis in human oral cancer HSC-3 cells. J. Dent. Res. 90, 168–174.
Yu, F.S., Yu, C.S., Chan, J.K., Kuo, H.M., Lin, J.P., Tang, N.Y., Chang, Y.H., Chung, J.G., 2006. The effects of emodin on the expression of cytokines and functions of leukocytes from Sprague–Dawley rats. In Vivo 20, 147–151.
Zhang, L., Lau, Y.K., Xi, L., Hong, R.L., Kim, D.S., Chen, C.F., Hortobagyi, G.N., Chang, C., Hung, M.C., 1998. Tyrosine kinase inhibitors, emodin and its derivative repress HER-2/neu-induced cellular transformation and metastasis-associated properties. Oncogene 16, 2855–2863.
Ziegler, D.S., Kung, A.L., 2008. Therapeutic targeting of apoptosis pathways in cancer. Curr. Opin. Oncol. 20, 97–103.